



Research paper

Substituted quinazolinones as kinase inhibitors endowed with anti-fibrotic properties

Giovanni Marzaro^{a,*}, Ignazio Castagliuolo^b, Giulia Schirato^b, Giorgio Palu'^b,
Martina Dalla Via^a, Adriana Chilin^a, Paola Brun^b^a Department of Pharmaceutical and Pharmacological Sciences, University of Padova, Via Marzolo 5, 35131 Padova, Italy^b Department of Molecular Medicine, University of Padova, Via Gabelli 63, 35121 Padova, Italy

ARTICLE INFO

Article history:

Received 11 January 2016

Received in revised form

17 March 2016

Accepted 18 March 2016

Available online 19 March 2016

Keywords:

Quinazolinones

Tyrosine kinases

Multi kinase inhibitors

Fibrosis

ABSTRACT

Some new 3-substituted quinazolinones were synthesized and evaluated as inhibitors of kinases involved in fibrogenic process. The compounds were tested against a panel of both tyrosine and serine–threonine kinases. The profile of selectivity of some representative compounds was investigated through molecular docking studies. The most interesting compounds were also evaluated *in vitro* as potential agents for the treatment of fibrotic diseases. Quinazolinone derivatives reduced proliferation and expression of genes involved in the fibrogenic process in hepatic stellate cells (HSCs) and intestinal subepithelial myofibroblasts (ISEMFs). Furthermore some compounds downregulated phosphorylation of p38MAPK. Our findings provide evidences that 3-substituted quinazolinones target multiple essential pathways of the fibrogenic process.

© 2016 Elsevier Masson SAS. All rights reserved.

1. Introduction

Protein kinases are ubiquitous enzymes devoted to the regulation of almost all cellular events. The kinases catalyze the transfer of a phosphate group from the ATP to specific substrate eventually leading to transduction and propagation of cellular signal [1]. Deregulated activity, mutation or over-expression of these enzymes have been correlated to cancer [2], chronic inflammatory disorders [3], diabetes [4], cardiovascular diseases [5] and hypertension [6]. According to the targeted amino acids, kinases are commonly grouped in two major families: the tyrosine kinases (TKs) and the serine–threonine kinases (STKs). Among the TKs, the epidermal growth factor receptor (EGFR), the type 2 vascular endothelial receptor (VEGFR2 or KDR), the type 1 fibroblast growth factor

receptor (FGFR1), and the cytoplasmic enzymes Abl1 and Src play crucial roles in cell proliferation as well as in cancer onset and progression [7]. On the other hand, the phosphatidylinositol-3 kinase (PI3K) is mainly a lipid kinase that, along with the mammalian target of rapamycin (mTOR), is included in the STK family. Indeed, by phosphorylation of serine or threonine containing proteins the mTOR/AKT/PI3K pathway controls several cellular functions including inflammatory responses and cancer development [8].

Remarkably, TKs and STKs-induced intracellular signals are important modulators of fibrogenic process in lung, liver, pancreas, heart, and gut. Fibrosis can occur during tissue repair or inflammation as a result of persistent activation of fibrogenic cells, which leads to aberrant extracellular matrix (ECM) deposition and progressive substitution of the normal parenchyma by scar tissue [9]. For instance, persistent liver injury and unrestrained inflammatory cascade lead to EGFR-mediated proliferation and migration of hepatic stellate cells (HSCs), the cellular population involved in the deposition of ECM in the liver [10]. In addition, release of specific growth factors triggers the synergistic activation of a number of protein kinase pathways that serve different biological roles related to fibrogenesis [11]. Inhibition of KDR by neutralizing monoclonal antibody ameliorated carbon tetrachloride induced hepatic fibrosis in mice not only by suppressing the neovascularisation but also by reducing the $\alpha 1(I)$ -procollagen mRNA expression in HSCs [12]. Likewise, preliminary randomized double-blind clinical trials

Abbreviations: CAN, cerium ammonium nitrate; CD, Crohn's Disease; COL1A1, prepro-alpha 1 collagen; DMF, dimethylformamide; ECM, extracellular matrix; EGFR, epidermal growth factor receptor; FGFR1, type 1 fibroblast growth factor receptor; FN1, fibronectin 1; HSC, hepatic stellate cells; ISEMF, intestinal subepithelial myofibroblasts; KDR, type 2 vascular endothelial receptor; mTOR, mammalian target of rapamycin; PDGFR, platelet-derived growth factor receptor; PI3K, phosphatidylinositol-3 kinase; STK, serine–threonine kinases; TFA, trifluoroacetic acid; TIMP1, tissue inhibitor of metalloproteinase 1; TK, tyrosine kinases; VEGFR2, type 2 vascular endothelial receptor.

* Corresponding author.

E-mail address: giovanni.marzaro@unipd.it (G. Marzaro).

indicate that sirolimus and everolimus, two mTOR inhibitors, induce remission in refractory Crohn's Disease (CD) by decreasing the number of intestinal subepithelial myofibroblasts (ISEMFs) and the expression of pro-fibrotic cytokines [13–15]. Currently, the pharmacological care in patients with tissue fibrosis relies on corticosteroids and immunosuppressant drugs but fibrosis-related consequences remain a major causes of morbidity and mortality [16].

The pivotal role of kinases as targets for novel drugs is clearly demonstrated by the huge amount of ATP-mimic kinase inhibitors, mainly TK inhibitors, developed in the last two decades [17]. The ATP-mimic kinase inhibitors belong to different chemical classes of compounds. However they share a common pharmacophore [17] that is generally composed by: *i*) a scaffold (mainly a nitrogen containing heterocycle) able to interact through an H-bond with the kinase *hinge region*; *ii*) a lipophilic moiety (mainly an aromatic or a heteroaromatic system) that occupy a pocket opened by the so called *gatekeeper* residue; *iii*) a spacer between the heterocycle and the hydrophobic moiety; *iv*) solvent exposed residues. As part of our novel bioactive compounds discovery projects [18–20] and due to our experience in quinazoline compounds [18,19,21], we decided to investigate whether it was possible to develop novel quinazolinone-based kinase inhibitors able to restrain the activation of fibrogenic cells. Quinazolinone compounds are endowed with a number of biological activities comprising antiviral [22], antitubercular [23], antimicrobial [24], antitubulin [25], antifolate [26], anticonvulsant [27], anti-inflammatory [28], antifibrotic [29] and anticancer [30–32] properties. Their kinase inhibitory activity however has not been extensively explored.

Herein we report the synthesis and the preliminary evaluation of several 3-substituted quinazolinones against a panel of kinases mainly involved in the fibrogenic process. The binding mode of several compounds with the target kinases was investigated by means of molecular docking studies. The anti-fibrotic activity of the compounds was assessed *in vitro*.

2. Results and discussion

2.1. Chemistry

The general structure of the novel compounds is reported in Fig. 1A.

The 3-substituted quinazolinone compounds are structurally related to another well known class of kinases inhibitors, the 4-anilinoquinazolines [34,35] (Fig. 1B), as demonstrated by the superimposition with erlotinib in its binding conformation with EGFR (Fig. 1C and D). According to our previous studies [19], the 6 and 7 positions of the quinazolinone scaffold were functionalized with dimethoxy functions or with fused dialkoxy rings, namely a dioxane and a dioxolane ring. The 3 position of the quinazolinone

was substituted with several lipophilic moieties (2-bromopyridine, biphenyl, halophenyl) linked to the quinazolinone nitrogen with a bridge of variable sizes and chemical properties (methylene, 2-hydroxyethylene, 2-oxoethylene). According to the type of substitution at the positions 6 and 7, the newly synthesized compounds were grouped in three classes (Table 1). All the compounds have been synthesized starting from the appropriate aniline derivatives through quinazoline intermediates, taking advantage of an already reported synthetic strategy [36] (Scheme 1).

Briefly, anilines **16a–c** were protected as carbamates, submitted to condensation with hexametylenetetramine in TFA under microwave irradiation and then to aromatization with potassium ferricyanide in hydroalcoholic KOH at reflux. The obtained quinazoline **18a–c** were oxidized with CAN in acetic acid to quinazolinones **19a–c** [18], which were finally condensed with the suitable halobenzyl derivatives, aryloxyrane or haloacetophenones and NaH in DMF under microwave irradiation give the final products **1–15**.

2.2. Kinase screening

To outline the profile of activity/selectivity, all the synthesized compounds were preliminarily screened for their ability to counteract the kinase activity of a selected panel of kinases (both TKs and STKs) involved in fibrosis [37–43]. Thus, in this study the synthesized compounds have been tested at 1 μ M against a panel of six tyrosine kinases and two serine–threonine kinases. Vatalanib (PTK787/ZK-22258, a poly-tyrosine kinase inhibitor endowed with anti-fibrotic and anti-neoplastic activities) [44,45] has been used as positive control. The results of the screening are summarized in Table 2.

Many compounds inhibited the activity of KDR or EGFR, though to a lower extent than vatalanib. The majority of these compounds (**6**, **10**, **11**, and **14**) were dual KDR and EGFR inhibitors, whereas compound **1** was a dual EGFR/PDGFR β (Platelet-Derived Growth Factor Receptor β -isoform) inhibitor. Moreover compounds **7** and **11** were also active against one of the tested STKs. All the compounds were inactive against the cytoplasmic kinases Abl1 and Src and the receptor kinase FGFR1.

2.3. Molecular docking

To rationalize the activity profile of some representative compounds, molecular modelling studies were performed. In particular we focused on compounds **1** (active against EGFR; inactive against KDR), **11** (active against KDR, EGFR and PI3K; inactive against mTOR) and **7** (active against mTOR; moderately active against PI3K).

As depicted in Fig. 2A, compound **1** was expected to interact through the *N*¹-quinazolinone nitrogen and the pyridine nitrogen with the hinge region residue M793 and with the gatekeeper T790

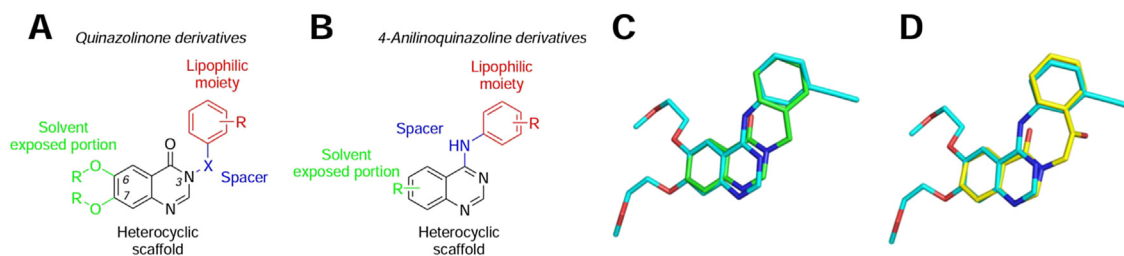
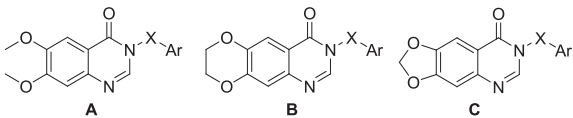


Fig. 1. (A) General structure of quinazolinone derivatives. (B) General structure of 4-anilinoquinazolinone kinase inhibitors. (C) Superimposition of the 3-benzylquinazolin-4-one scaffold (green carbon sticks) and erlotinib (cyan carbon sticks). (D) Superimposition of the 3-(benzoylmethyl)quinazolin-4-one scaffold (yellow carbon sticks) and erlotinib (cyan carbon sticks). The tridimensional structure of erlotinib was extracted by the crystallographic complex with EGFR (PDB ID: 1M17) [33]. (For interpretation of the references to colour in this figure legend, the reader is referred to the web version of this article.)

Table 1
Structures of the synthesized compounds.



Compd	Series	X	Ar
1	A	-CH ₂ -	
2	A	-CH ₂ -	
3	A	-CH ₂ -	
4	A	-CH ₂ -	
5	A	-CH ₂ CO-	
6	A	-CH ₂ CH(OH)-	
7	B	-CH ₂ -	
8	B	-CH ₂ -	
9	B	-CH ₂ -	
10	B	-CH ₂ CO-	
11	B	-CH ₂ CO-	
12	B	-CH ₂ CH(OH)-	
13	C	-CH ₂ -	
14	C	-CH ₂ -	
15	C	-CH ₂ -	

of EGFR respectively. No consistent binding mode for compound **1** in KDR was obtained. Probably, the presence of the V916 as gate-keeper in KDR was detrimental for the activity: when the pose obtained for compound **1** in EGFR was inserted in KDR a clash between the valine and the lipophilic moiety was observed (Fig. 2B).

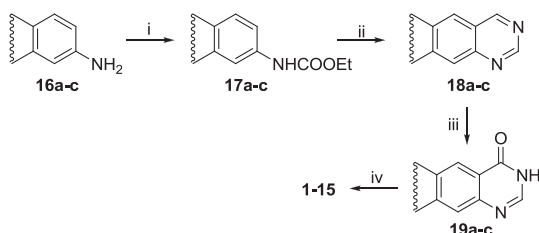
The presence of a longer bridge with H-bond acceptor feature in compound **11** was probably the key to achieve dual EGFR/KDR inhibition (Fig. 3). Again, the *N*¹-quinazolinone nitrogen was expected to form an H-bond with the hinge residues (M790 in EGFR, Fig. 3A; C918 in KDR, Fig. 3B). In the case of EGFR, an additional H-bond between the alcoholic function of T790 and the carbonyl of **11** was suggested by molecular docking, whereas in KDR the bromophenyl function probably established lipophilic interaction with the gate-keeper (V916).

Notably, a similar behaviour was found also for compound **5** and **10**, bearing the same CH₂C=O bridge (data not shown).

Besides being a dual EGFR/KDR inhibitor, compound **11** was also able to inhibit PI3K while it was inactive against the other tested STK, mTOR. On the contrary, the shorter bridge in compounds **7** and **8** led to compounds endowed with moderate dual mTOR/PI3K inhibitory activity. As depicted in Fig. 4, **7** (Fig. 4A) and **11** (Fig. 4B) showed comparable binding modes in PI3K. Docking studies suggested that the dioxane oxygens could establish H-bonds with the hinge residue V848, the *N*¹-quinazolinone nitrogen atoms could interact with the K799 and the lipophilic moieties may be involved in T-shaped arene–arene interactions with the W781 aromatic side chains.

Conversely, in mTOR kinase, compound **7** was expected to interact with the hinge residue V2240 through an H-bond, with the W2239 through a T-shaped arene–arene interaction and with the DFG-motif (Fig. 5A). A similar pose was not obtained for compound **11**. Indeed, the alignment of compound **11** on the pose obtained for compound **7** in mTOR revealed two clashes between the carbonyl in the bridge and the W2239 and between the bromine atom and the I2163 side chain (Fig. 5B).

Finally, we used molecular docking studies also to investigate the differences in potencies of compounds **1**, **3** and **4** against EGFR. Indeed, very small variation in structures (compounds mainly differed for the relative position of the bromine atom and for the presence of a pyrimidine in place of a phenyl function at position 3) caused quite high differences. As shown in Fig. 6A, there were probably no differences in binding modes for compounds **1** and **3**. Hence, the lower activity of **3** could be ascribed to the lack of interaction with the T790 (due to the absence of the nitrogen atom in the benzyl portion) rather than to the bromine atom position. On



^aReagents and conditions: (i) ClCOOEt, TEA, THF, rt, 30 min; (ii) 1. HMTA, TFA, MW, 110 °C, 10 min. 2. K₃Fe(CN)₆, KOH 10%, EtOH/H₂O 1/1, reflux, 4 h; (iii) CAN, AcOH, H₂O, rt, 5 min; (iv) 2-bromo-3-bromomethylpyridine (**1**) or 3-phenyl-benzylbromide (**2**, **14**) or 3-bromobenzylbromide (**3**, **8**) or 4-bromobenzylbromide (**4**, **9**, **13**) or 4-phenylbenzylchloride (**7**, **15**) or 2,4'-dibromoaceto-phenone (**5**, **10**) or 2,3'-dibromo-acetophenone (**11**), or 2-(4-bromophenyl)oxirane (**6**) or 2-(3-chlorophenyl)oxirane (**12**), NaH, anhydrous DMF, MW, 120 °C, 5 min.

Scheme 1. General strategy for the synthesis of quinazolinone derivatives as kinase inhibitors^a.

Table 2
Kinase inhibition profile.

Compd	% inhibition ([I] = 1 μ M) against isolated kinases ^a							
	KDR	EGFR	FGFR1	Abl1	Src	PDGFR β	mTOR	PI3K
1	24	49	13	0	3	37	30	25
2	33	16	13	0	0	4	34	21
3	31	35	11	0	0	22	18	15
4	25	23	14	0	0	0	25	0
5	53	33	7	0	4	1	17	0
6	44	53	8	0	0	0	33	5
7	45	29	10	0	5	13	37	25
8	12	23	7	0	0	0	28	28
9	12	31	1	0	0	1	13	0
10	35	43	18	0	0	1	23	17
11	36	47	18	0	0	4	2	35
12	26	38	5	1	0	0	1	0
13	27	0	1	0	0	45	17	7
14	35	41	8	0	0	0	0	0
15	25	0	6	4	0	4	10	0
Vat	58	67	31	25	16	72	49	18

^aThe results are expressed as mean of three independent experiments. See Supplementary Data for all the measured values. Strong inhibition ($\geq 50\%$) is highlighted by black boxes; good inhibition ($\geq 35\%$) is highlighted by grey boxes; weak inhibition ($< 35\%$) is not highlighted. Vat: vatalanib.

the contrary, docking studies suggested a worse complementarity with the ATP pocket for compound **4** (Fig. 6B), probably caused by the hindrance of the *para*-bromine atom.

2.4. *In vitro* anti-fibrotic activity

As many substituted quinazolinones are endowed with good/strong inhibition activity towards kinases involved in the fibrogenic process (Table 2), we decided to assess the biological effect of the active compounds in modulating the activation of fibrogenic cells, namely HSCs and ISEMFs. Primary cells were isolated from human liver or gut specimens and cultured in plastic support to induce *in vitro* fibrogenic activation. As reported in Fig. 7, at 1 μ M compounds **6**, **7**, **10**, **11**, and **14** were the most effective in reducing the mRNA levels specific for COL1A1 in HSCs and ISEMFs. The mRNA transcript levels specific for FN1 and TIMP1 were decreased also by compounds **1** and **5**. Noteworthy, compounds **6**, **7**, **10**, **11**, and **14** showed a unique profile of activity in the series since they were able to inhibit KDR with strong/good potency and at least another kinase (Table 2). Compounds **1** and **5** effectively reduced the mRNA expression levels of TIMP1 and FN1 in pathological samples (*i.e.* ISEMFs cultured from patients suffering from Crohn's disease) with poor effect on myofibroblasts obtained from healthy subjects in which the fibrogenic activation is probably less important. For all the tested genes, the reduction in the mRNA expression was comparable to one reported for vatalanib. Finally, compounds endowed

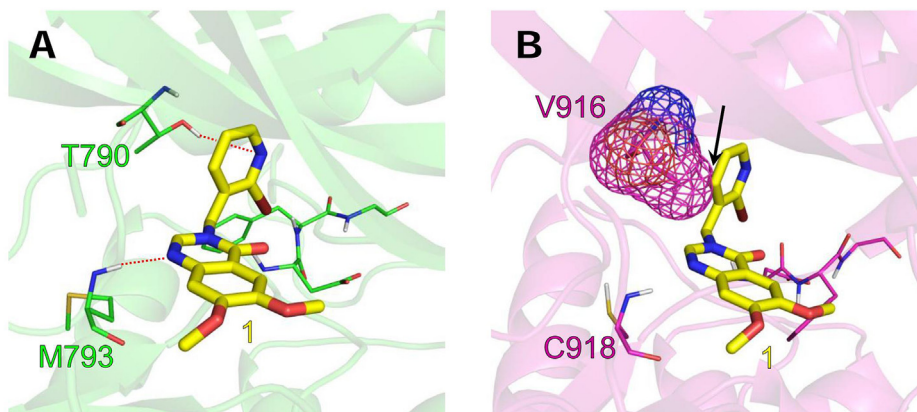


Fig. 2. (A) Binding mode proposed for **1** in EGFR. (B) Clash (black arrow) between **1** and V916 in KDR (V916 is represented as mesh surface). In both cases, the kinase hinge region is on the left side of the pictures, while the kinase solvent accessible region is on the right side.

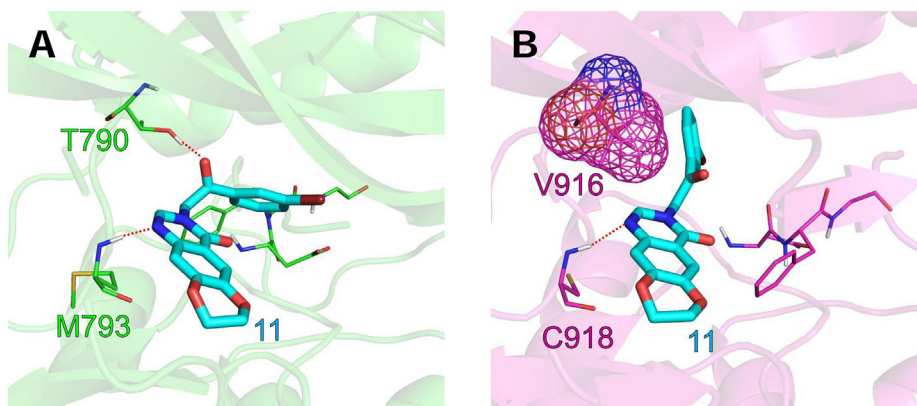


Fig. 3. (A) Binding mode proposed for **11** in EGFR. (B) Binding mode proposed for **11** in KDR (V916 is represented as mesh surface). In both cases, the kinase hinge region is on the left side of the pictures, while the kinase solvent accessible region is on the right side.

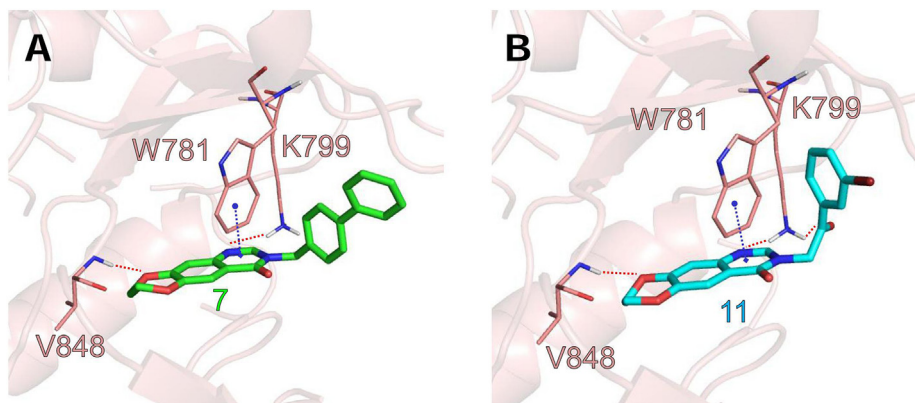


Fig. 4. (A) Binding modes proposed for **7** in PI3K. (B) Binding mode proposed for **11** in PI3K. In both cases, the kinase hinge region is on the left side of the pictures, while the kinase solvent accessible region is on the right side.

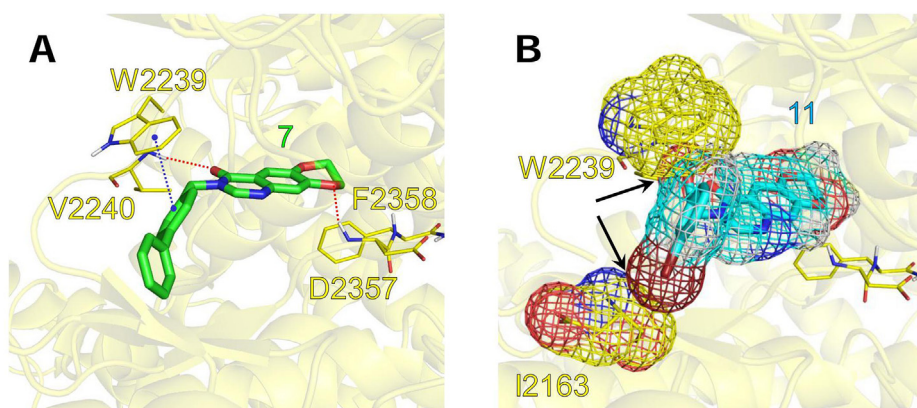


Fig. 5. (A) Binding proposed for **7** in mTOR. (B) Clashes (black arrows) between **11** and W2239 and I2163 in mTOR (**11**, W2239 and I2163 are depicted as mesh surfaces). In both cases, the kinase hinge region is on the left side of the pictures, while the kinase solvent accessible region is on the right side.

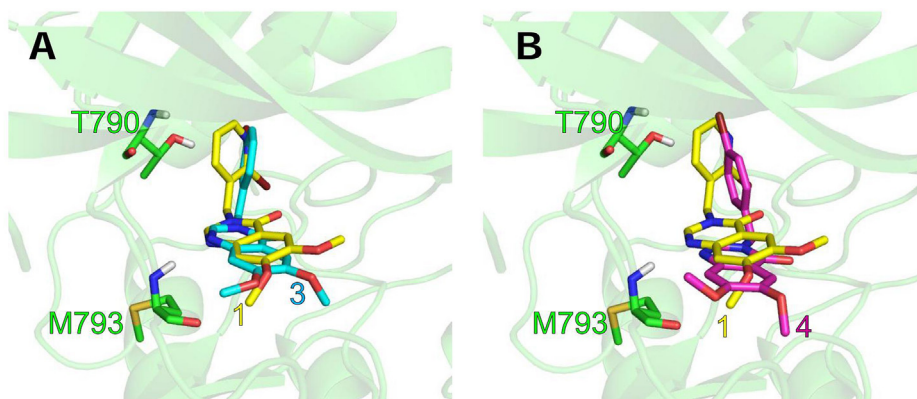


Fig. 6. (A) Comparison between the binding modes suggested by docking studies for **1** (yellow carbon sticks) and **3** (cyan carbon sticks) in EGFR. (B) Comparison between binding modes of **1** (yellow carbon sticks) and **4** (pink carbon sticks) in EGFR. In both cases, the kinase hinge region is on the left side of the pictures, while the kinase solvent accessible region is on the right side. (For interpretation of the references to colour in this figure legend, the reader is referred to the web version of this article.)

with weak inhibitor activity (**3**, **12**, **13**) did not significantly reduce the expression of genes involved in the fibrogenic process.

Compounds **1**, **6**, and **13** also inhibited proliferation in HSCs and ISEMFs. Consistent with previous reports, VEGF induces proliferation in HSCs [46]. As reported in Fig. 8, treatment of cells with 1 μ M for 72 h significantly decreased VEGF-induced proliferation. The effect was more evident in cells treated with compounds **1** and **13**,

the only quinazolinone derivatives endowed with good inhibition of PDGFR.

Most important, the treatment for 72 h with compounds at 1 μ M did not compromise cell viability (Fig. 9). On the contrary, under the same conditions vatalanib reduced cell viability, as previously reported [47].

The anti-fibrogenic and anti-proliferative effects of compounds

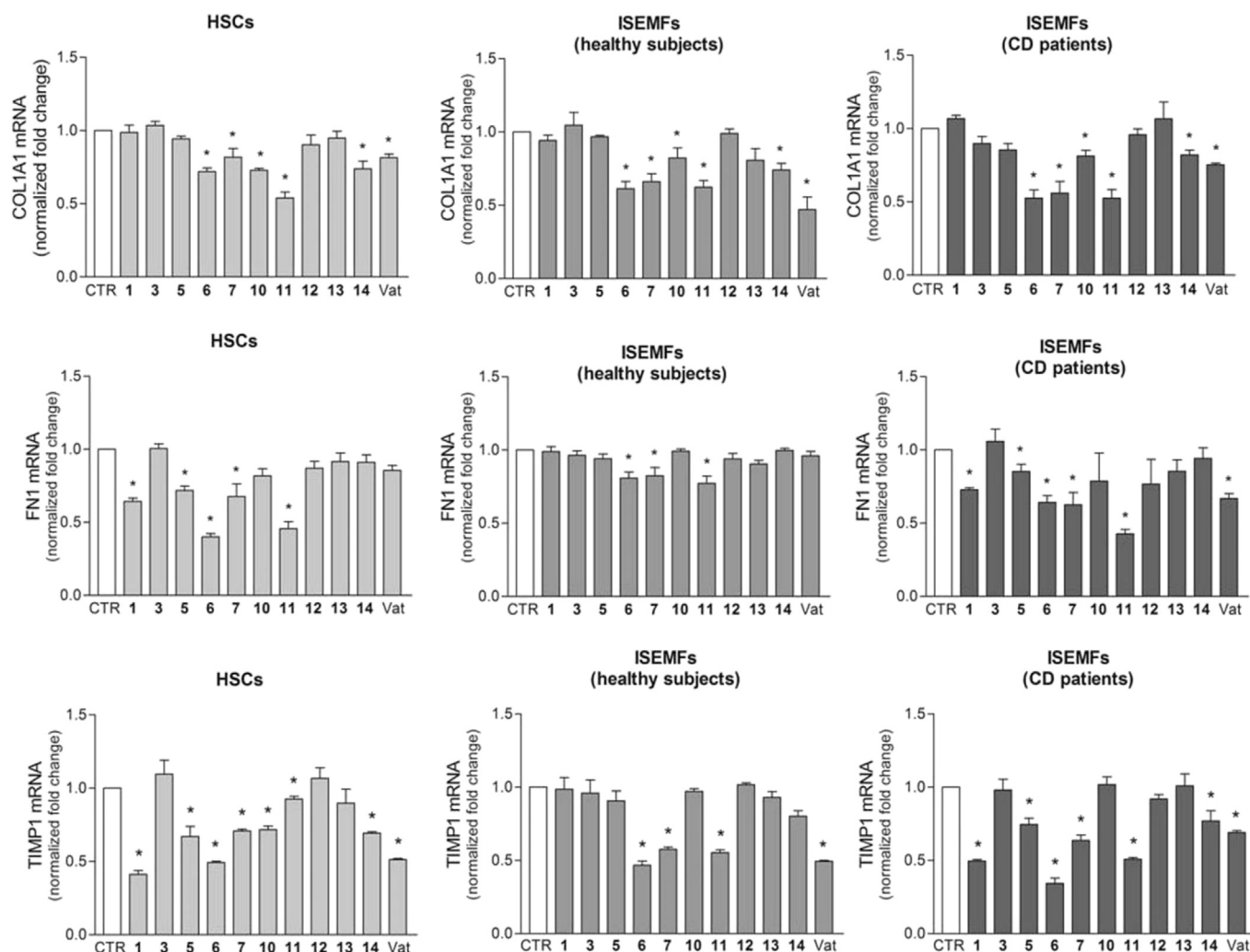


Fig. 7. Expression levels of mRNA transcripts specific for prepro- $\alpha 1$ collagen (COL1A1), fibronectin (FN1), and tissue inhibitor of metalloproteinase 1 (TIMP1) assessed by quantitative RT-PCR on hepatic stellate cells (HSCs) and intestinal subepithelial myofibroblasts (ISEMFs) cultured from specimens obtained by healthy subjects and patients suffering from Crohn's disease (CD). Data are reported as mean \pm SE. * denotes $P < 0.05$ vs untreated, control cells (CTR). Vat: vatalanib.

1, **6**, and **11** were associated with reduced phosphorylation of p38 MAPK. Thus, phosphorylation of p38MAPK is augmented in activated HSCs mediating the upregulation of COL1A1 mRNA levels [48]. Indeed, phospho-p38MAPK levels mainly decreased in HSCs treated for 4 h with compounds **1**, **6** and **11** at 1 μ M as compare to untreated cells (Fig. 10). Similar results were obtained in ISEMFs cultured from patients suffering from Crohn's disease (data not shown).

3. Conclusions

The evaluation of kinase inhibitors bearing the quinazolinone core has not yet been extensively studied, although this scaffold is present in a number of biologically active compounds. In this work the synthesis and the preliminary biological evaluation of quinazolinone derivatives as kinase inhibitors have been described. The synthesized compounds have been tested towards a panel of six tyrosine kinases and two serine–threonine kinases. The profile of selectivity of some representative compounds has been rationalized through molecular docking studies, furnishing useful suggestions for further development of this class of compounds.

The kinase inhibition profile evaluated by *in vitro* assay (Table 2) prompted us to investigate the anti-fibrotic properties of

quinazolinone derivatives. Our data revealed that the synergistic inhibition of EGFR and KDR efficaciously reduced the levels of mRNA transcripts involved in the fibrogenic activation of both HSCs and ISEMFs, the cell populations mainly involved in the fibrosis of liver and gut, respectively. Indeed, compounds **6**, **10**, **11** and **14**, showing the dual EGFR/KDR inhibitory activity, significantly reduced COL1A1 mRNA expression as compare to non-treated *in vitro* activated cells to an extent comparable to or even greater than vatalanib. Previous studies reported the involvement of EGFR and KDR in the regulation of HSCs [10,12] but to our knowledge this is the first time that dual inhibitors of TKs efficaciously control expression of fibrogenic genes. The simultaneous inhibition of KDR and EGFR however is not mandatory for the anti-fibrotic effect. Indeed, compounds **1**, **5**, and **7** revealed different gene-related and cellular specific effects. In particular, compound **7** endowed with dual KDR/mTOR inhibitory activity, significantly downregulated the expression of pro-fibrogenic genes. Thus, several soluble factors and signalling pathways are central to the fibrotic process. Besides EGFR and KDR, PDGFR has been reported as the most potent proliferative factor toward HSCs and myofibroblasts [49]. Because of their combined role in fibrosis, inhibition of both proliferation and fibrogenesis is an attractive target for antifibrotic therapy. Among our synthesized quinazolinone derivatives only compound **1**

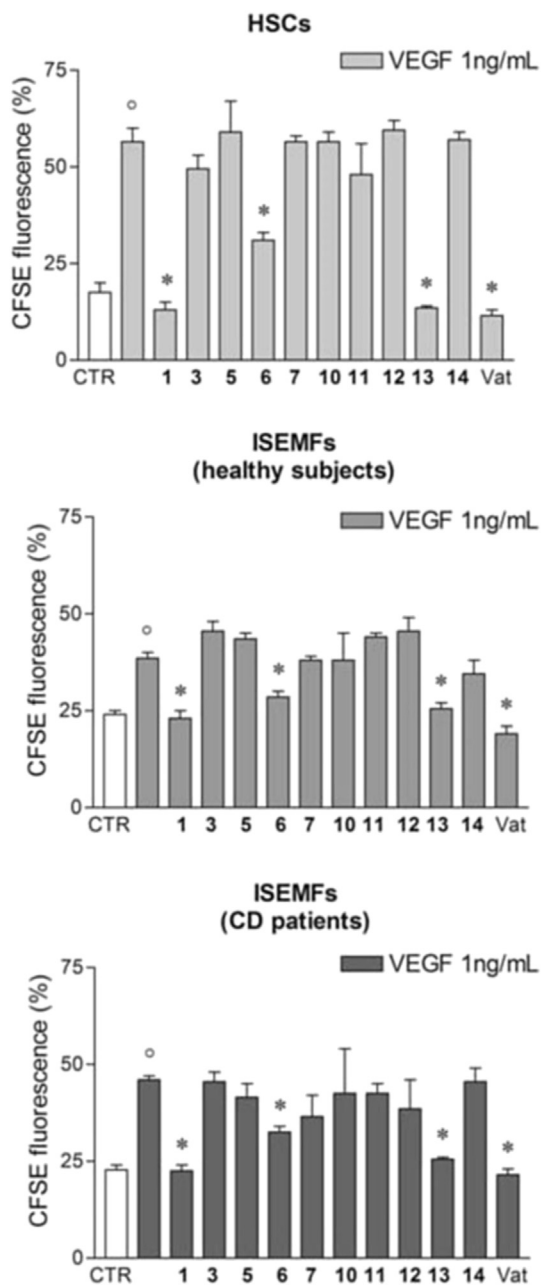


Fig. 8. Cell proliferation assessed as carboxyfluorescein diacetate succinimidyl ester (CFSE) positive cells (percentage). HSCs and ISEMFs were treated with 1 ng/ml VEGF and compounds for 72 h. Fluorescence was then evaluated by FACS analysis. Data are reported as mean \pm SE. $^{\circ}$ denotes $P < 0.05$ vs untreated, control cells (CTR). * denotes $P < 0.05$ vs VEGF-treated cells. Vat: vatalanib.

inhibits both PDGFR and EGFR (Table 2). Consistently, compound **1** reported good anti-fibrotic activity, reducing FN1 and TIMP1 mRNA transcript levels and also inhibited VEGF-induced cell proliferation. However, even if at lower extent compound **6** reported anti-proliferative activity, too, proving that quinazolinone derivatives inhibit activated fibrogenic cells by complex mechanisms. Indeed, compounds **1**, **6**, and **11** exert their anti-fibrotic and anti-proliferative effects on p38MAPK pathway although we can not exclude other intracellular signaling cascades.

On the basis of the acquired data and of the docking studies, novel compounds with improved inhibitory activity against STKs will be synthesized, with the aim to strengthen the anti-fibrotic

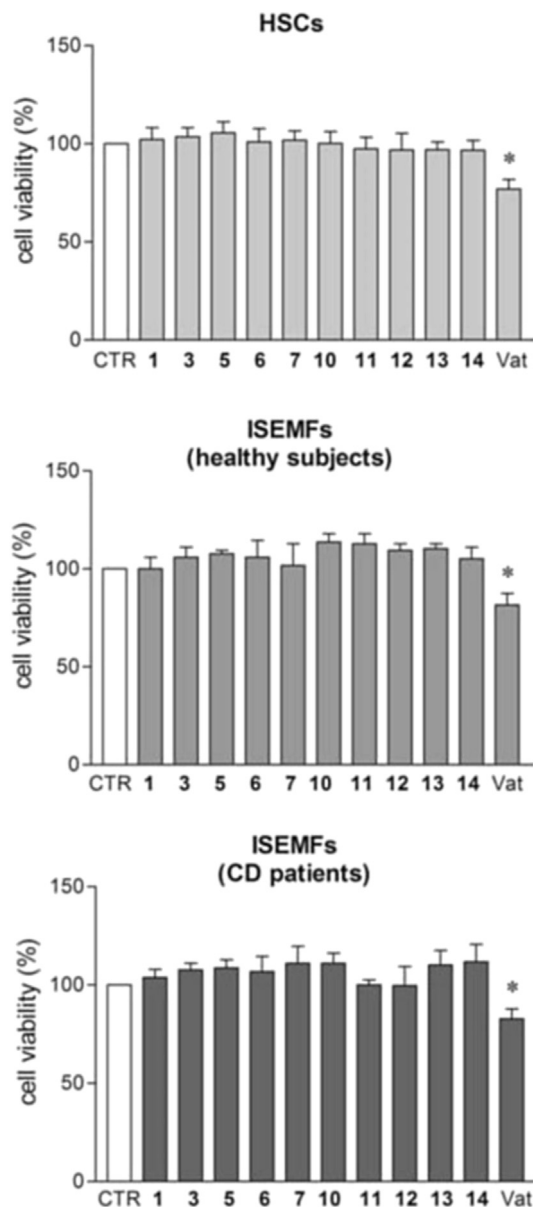


Fig. 9. Percentage of vital HSCs and ISEMFs following treatment with compounds for 72 h. Data are reported as mean \pm SE. * denotes $P < 0.05$ vs untreated, control cells (CTR). Vat: vatalanib.

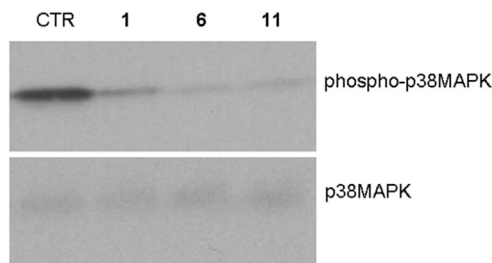


Fig. 10. Inhibition of p38MAPK phosphorylation assessed by western blot analysis in HSCs untreated (CTR) or treated for 4 h with compounds 1 μ M.

properties of quinazolinone derivatives. Fully exhaustive relationship between kinases inhibition profile and biological activity is however not derivable mainly because i) the expression of the

different ECM proteins is driven by several intracellular pathways and *ii*) different kinases are specifically elicited in distinct cell populations (*i.e.* HSCs and ISEMFs) as well as at different step of the fibrogenic process (compare effects on ISEMFs from healthy subjects and patients suffering for Crohn's disease). Indeed, a complex network of extracellular factors (*e.g.* endocrine system, metabolism, growth factor and metalloproteinase secretion) characterizes fibroblast activation and ECM deposition in every tissue-related fibrogenic process [50,51]. The acquired data indicate compounds **1**, **6**, and **11** as novel promising anti-fibrotic compounds endowed with multiple kinases inhibitory properties. The synthesis of novel compounds as well as a more exhaustive biological investigation on this novel class of multi-kinase inhibitors is in progress. Overall, our data suggest that the quinazolinone is an attractive scaffold for the development of novel inhibitors of kinases involved in the fibrogenic process.

4. Experimental

4.1. Chemistry

See [Supplementary Data](#) for general synthetic methods, for the synthesis of 2-bromo-3-bromethylpyridine and for the analytical details (mp, NMR, HRMS, elemental analyses) of all compounds. Purity of all tested compounds was determined by elemental analyses and was found equal or more than 95%. Compounds **19a** [21] and **19b-c** [18] were synthesized as previously reported.

General procedure for quinazolinones 1–15. A mixture of quinazolinone **19a** [21] or **19b-c** [18] (1.0 mmol) and NaH in DMF was maintained under N₂ for 5 min. The appropriate haloderivative or aryloxirane was added (1.0 mmol) and the mixture was microwave irradiated at 120 °C (power 250 W; hold time 5 min). After cooling, the mixture was poured in sat. NH₄Cl solution (30 mL) and the obtained precipitate were collected by filtration. The solid was purified by crystallization to give the title compounds (yields 10–52%).

4.2. Computational methodologies

The computational experiments were performed on a 4 CPUs (Intel Core2 Quad CPU Q9550 @ 2.83 GHz) ACPI ×64 Linux workstation (operating system: Ubuntu ver. 12.04). Protein structures were handled with Chimera 1.5.3 software [52]. The structures of the quinazolinone compounds were prepared using MarvinSketch 5.5.0.1 software [53] and OpenBabel 2.2.3 softwares [54]. The docking studies were conducted with AutoDock 4.2 software [55] as previously reported [19]. Further details are given in [Supplementary Data](#).

4.3. Biology

4.3.1. *In vitro* kinase assays

Synthesized compounds were tested *in vitro* for inhibition of a panel of TKs and STKs, as previously reported [19]. See [Supplementary Data](#) for a detailed description.

4.3.2. Cell isolation and culture

Human hepatic stellate cells (HSCs) were freshly isolated from non-pathological fragments of liver tissue collected during surgical procedures. Samples were processed separately and HSCs were cultured as previously described [56]. Briefly, following digestion with collagenase and pronase, HSCs were isolated by centrifugation over a gradient of Percoll (Amersham Biosciences, Sweden) and cultured in DMEM containing 10% vol/vol fetal bovine serum, 2 mM L-glutamine, 100 U/ml penicillin and 100 µg/ml streptomycin, (all

provided by Gibco, Milan, Italy). Purity of cultured HSCs was assessed by immunocytochemistry using anti- α SMA antibody (Sigma).

Human intestinal subepithelial myofibroblasts (ISEMFs) were isolated from non-pathological colonic biopsies collected during colonoscopy for cancer screening and from patients with Crohn's disease collected during routine follow-up endoscopy program. Tissue samples were processed separately. Biopsies were diced and digested for 30 min at 37 °C in collagenase (0.25 mg/ml, Sigma). Recovered cells were suspended in DMEM with 20% vol/vol FBS, 2 mM L-glutamine, 1 mM sodium pyruvate, 0.1 mM nonessential amino acids, 100 U/ml penicillin, 100 µg/ml streptomycin and 2 ng/ml fungizone (Gibco). Purity of cultured ISEMFs was ascertained by fluorescence-activated cell sorting (FACS) analysis using anti-CD90 antibody (ImmunoTools, Germany). HSCs and ISEMFs were cultured at 37 °C in a 5% CO₂ humidified incubator. At confluence, cells were detached using 0.05% Trypsin-EDTA (Gibco). The study protocol followed the principles expressed in the Declaration of Helsinki and was approved by the Ethical Committee of the University Hospital of Padova. Each patient was provided with detailed information about the study aims and protocols, and gave their written, informed consent.

4.3.3. RNA isolation and quantitative polymerase chain reaction

HSCs and ISEMFs were cultured in 6 well plates and treated for 24 h with 1 µM of test compounds or vatalanib. Total RNA was extracted using the SV total RNA isolation system (Promega, Italy) according to the manufacturer's instructions. Contaminating DNA was removed by DNase I treatment (Promega). cDNA was synthesized using 2 µg RNA as template, random hexamer primers and MuLV Reverse Transcriptase (Applied Biosystems, Milan, Italy). Gene expression was evaluated by quantitative polymerase chain reactions (qPCR) using ABI Prism 7700 Sequence Detection System (Applied Biosystems), TaqMan qPCR Master Mix (Applied Biosystems), and specific oligonucleotides and probes (Universal Probe Library system, UPL, Roche Applied Science, Monza, Italy) for prepro-alpha 1 collagen (COL1A1), fibronectin 1 (FN1), and tissue inhibitor of metalloproteinase 1 (TIMP1). The expression of the target gene was normalized to the level of the housekeeping gene 18S ribosomal RNA (18SrRNA). Experiments were performed in triplicate for each isolated cell batch. The relative changes in gene expression were analyzed using the $\Delta\Delta$ CT method. Oligonucleotides and probes are reported in [Supplementary Data](#).

4.3.4. Proliferation assay

HSCs and ISEMFs were incubated at 37 °C for 10 min in pre-warmed PBS containing 0.1% vol/vol BSA (Sigma) and 25 mM carboxyfluorescein diacetate succinimidyl ester (CFSE, Molecular Probe, Invitrogen). Staining was quenched by adding 5 volumes of ice-cold culture media. Sixteen hrs later the cells were washed and treated with 1 µM compounds or vatalanib for 72 h. Cell proliferation was evaluated by the partitioning of fluorescent dye between daughter cells using BD FACS-Calibur flow cytometer. Experiments were performed in duplicate for each isolated cell batch. Results were analyzed using the WinMDI 2.9 (Windows Multiple Document Interface for Flow Cytometry) program.

4.3.5. Cell viability assay

To evaluate cell viability, HSCs and ISEMFs were seeded into 96-well plates at 2×10^3 cells/well. Cells were then exposed for 72 h to 1 µM tested compounds or vatalanib and finally added with 3-(4,5-dimethylthiazol-2-yl)-2,5-dimethyltetrazolium bromide (MTT, 0.50 mg/ml, Sigma) for 4 h. Formazan crystals were dissolved in 10% w/vol SDS containing 0.01 M HCl. Optical densities were measured at 450 nm using a microplate reader (Sunrise, Tecan; Switzerland).

Experiments were performed in triplicate for each isolated cell batch and cell viability was expressed as a percentage relative to respective untreated cells.

4.3.6. Western blotting

HSCs and ISEMFS isolated from gut specimens of patients suffering from Crohn's disease were treated for 4 h with compounds at 1 μ M. For Western blot analysis total proteins from cultured cells were extracted in RIPA buffer (150 mM NaCl, 50 mM Tris–HCl, 0.25% wt/vol sodium deoxycholate, 0.1% Nonidet P-40, 100 μ M NaVO₄, 1 mM NaF, 1 mM phenylmethylsulfonyl fluoride, 10 μ g/ml aprotinin, 10 μ g/ml leupeptin). Particulate material was removed by centrifugation. Proteins were separated with 10% SDS PAGE and then transferred to nitrocellulose membranes (BioRad, Italy). Membranes were probed with phospho-p38 MAP Kinase antibody (Cell Signaling) and then incubated with anti-rabbit HRP-conjugated secondary antibodies. Immune complexes were visualized using enhanced chemiluminescence (Millipore). Membranes were then re-probed with p-38 MAP Kinase antibody as loading control. Experiments were performed in duplicate. Images were captured using Hyper Film MP (GE Healthcare).

4.3.7. Statistical analysis

Statistical analysis was performed using GraphPad Prism 3.03 software (San Diego, California, USA). One-way analysis of variance followed by the Bonferroni post-hoc test was used to compare multiple experimental groups. *P* values < 0.05 were considered statistically significant.

Acknowledgment

The present work has been carried out with the financial support of the University of Padova “Progetto di Ricerca di Ateneo 2008” CPDA084954/08 to A.C. and “Progetto Giovani Studiosi 2012” to G.M.. M.D.V. thanks the Fondazione Cariparo for a PhD student grant.

Appendix A. Supplementary data

Supplementary data related to this article can be found at <http://dx.doi.org/10.1016/j.ejmech.2016.03.053>.

Author contributions

The manuscript was written through contributions of all authors. All authors have given approval to the final version of the manuscript.

References

- [1] G. Manning, D.B. Whyte, R. Martinez, T. Hunter, S. Sudarsanam, The protein kinase complement of the human genome, *Science* 298 (2002) 1912–1934.
- [2] C. Tsatsanis, D.A. Spandidos, The role of oncogenic kinases in human cancer (Review), *Int. J. Mol. Med.* 5 (2000) 583–590.
- [3] M. Gaestel, A. Mengel, U. Bothe, K. Asadullah, Protein kinases as small molecule inhibitor targets in inflammation, *Curr. Med. Chem.* 14 (2007) 2214–2234.
- [4] D. Koya, G.L. King, Protein kinase C activation and the development of diabetic complications, *Diabetes* 47 (1998) 859–866.
- [5] K.P. Nunes, C.S. Rigsby, R.C. Webb, RhoA/Rho-kinase and vascular diseases: what is the link? *Cell. Mol. Life Sci.* 67 (2010) 3823–3836.
- [6] A. Wirth, Rho kinase and hypertension, *Biochim. Biophys. Acta* 1802 (2010) 1276–1284.
- [7] M.K. Paul, A.K. Mukhopadhyay, Tyrosine kinase - role and significance in Cancer, *Int. J. Med. Sci.* 1 (2004) 101–115.
- [8] D. Morgensztern, H.L. McLeod, PI3K/Akt/mTOR pathway as a target for cancer therapy, *Anticancer Drugs* 16 (2005) 797–803.
- [9] G.C. Gurtner, S. Werner, Y. Barrandon, M.T. Longaker, Wound repair and regeneration, *Nature* 453 (2008) 314–321.
- [10] C.Q. Yang, M. Zeisberg, B. Mosterman, A. Sudhakar, U. Yerramalla, K. Holthaus, L.M. Xu, F. Eng, N. Afdhal, R. Kalluri, Liver fibrosis: insights into migration of hepatic stellate cells in response to extracellular matrix and growth factors, *Gastroenterology* 124 (2003) 147–159.
- [11] M. Presta, P. Dell'Era, S. Mitola, E. Moroni, R. Ronca, M. Rusnati, Fibroblast growth factor/fibroblast growth factor receptor system in angiogenesis, *Cytokine Growth Factor Rev.* 16 (2005) 159–178.
- [12] H. Yoshiji, S. Kuriyama, J. Yoshii, Y. Ikenaka, R. Noguchi, D.J. Hicklin, Y. Wu, K. Yanase, T. Namisaki, M. Yamazaki, H. Tsujinoue, H. Imazu, T. Masaki, H. Fukui, Vascular endothelial growth factor and receptor interaction is a prerequisite for murine hepatic fibrogenesis, *Gut* 52 (2003) 1347–1354.
- [13] B. Osman, S. Akool el, A. Doller, R. Muller, J. Pfeilschifter, W. Eberhardt, Differential modulation of the cytokine-induced MMP-9/TIMP-1 protease-antiprotease system by the mTOR inhibitor rapamycin, *Biochem. Pharmacol.* 81 (2011) 134–143.
- [14] J. Dumortier, M.G. Lapalus, O. Guillaud, G. Poncet, M.C. Gagnieu, C. Partensky, J.Y. Scoazec, Everolimus for refractory Crohn's disease: a case report, *Inflamm. Bowel. Dis.* 14 (2008) 874–877.
- [15] D.C.O. Massey, F. Bredin, M. Parkes, Use of sirolimus (rapamycin) to treat refractory Crohn's disease, *Gut* 57 (2008) 1294–1296.
- [16] J.P. Iredale, Cirrhosis: new research provides a basis for rational and targeted treatments, *Bmj* 327 (2003) 143–147.
- [17] J. Zhang, P.L. Yang, N.S. Gray, Targeting cancer with small molecule kinase inhibitors, *Nat. Rev. Cancer* 9 (2009) 28–39.
- [18] A. Chilin, M.T. Conconi, G. Marzaro, A. Guiotto, L. Urbani, F. Tonus, P. Parnigotto, Exploring epidermal growth factor receptor (EGFR) inhibitor features: the role of fused dioxigenated rings on the quinazoline scaffold, *J. Med. Chem.* 53 (2010) 1862–1866.
- [19] M.T. Conconi, G. Marzaro, L. Urbani, I. Zanusso, R. Di Liddo, I. Castagliuolo, P. Brun, F. Tonus, A. Ferrarese, A. Guiotto, A. Chilin, Quinazoline-based multi-tyrosine kinase inhibitors: synthesis, modeling, antitumor and antiangiogenic properties, *Eur. J. Med. Chem.* 67 (2013) 373–383.
- [20] V. Gandin, A. Ferrarese, M. Dalla Via, C. Marzano, A. Chilin, G. Marzaro, Targeting kinases with anilinoquinazolines: discovery of N-phenyl-N'-[4-(pyrimidin-4-ylamino)phenyl]urea derivatives as selective inhibitors of class III receptor tyrosine kinase subfamily, *Sci. Rep.* 5 (2015) 16750.
- [21] G. Marzaro, A. Guiotto, G. Pastorini, A. Chilin, A novel approach to quinazolin-4(3H)-one via quinazoline oxidation: an improved synthesis of 4-anilinoquinazolines, *Tetrahedron* 66 (2010) 962–968.
- [22] Z. Wang, M. Wang, X. Yao, Y. Li, J. Tan, L. Wang, W. Qiao, Y. Geng, Y. Liu, Q. Wang, Design, synthesis and antiviral activity of novel quinazolinones, *Eur. J. Med. Chem.* 53 (2012) 275–282.
- [23] J. Kunes, J. Bazant, M. Pour, K. Waisser, M. Slosarek, J. Janota, Quinazoline derivatives with antitubercular activity, *Farmaco* 55 (2000) 725–729.
- [24] M.A. Khalil, N.S. Habib, Synthesis of thiazidazol derivatives of 4(3H)-quinazolinone as potential antimicrobial agents, *Farm. Sci.* 42 (1987) 973–978.
- [25] M.J. Hour, K.T. Lee, Y.C. Wu, C.Y. Wu, B.J. You, T.L. Chen, H.Z. Lee, A novel antitubulin agent, DPQZ, induces cell apoptosis in human oral cancer cells through Ras/Raf inhibition and MAP kinases activation, *Arch. Toxicol.* 87 (2013) 835–846.
- [26] S.T. Al-Rashood, G.S. Hassan, S.M. El-Messery, M.N. Nagi, S.E. Habib el, F.A. Al-Omary, H.I. El-Subbagh, Synthesis, biological evaluation and molecular modeling study of 2-(1,3,4-thiadiazolyl)-thio and 4-methyl-thiazolyl-thio-quinazolin-4-ones as a new class of DHFR inhibitors, *Bioorg. Med. Chem. Lett.* 24 (2014) 4557–4567.
- [27] N. Das, D. Garabadu, A. Banerjee, S. Krishnamurthy, S. Shrivastava, Synthesis and pharmacological evaluation of some N3-aryl/heteroaryl-substituted 2-(2-chlorostyryl)-6,7-dimethoxy-quinazolin-4(3H)-ones as potential anticonvulsant agents, *Med. Chem. Res.* 23 (2014) 4167–4176.
- [28] D.S. Brown, J.G. Cumming, P. Bethel, J. Finlayson, S. Gerhardt, I. Nash, R.A. Pauptit, K.G. Pike, A. Reid, W. Snelson, S. Swallow, C. Thompson, The discovery of N-cyclopropyl-4-methyl-3-[6-(4-methylpiperazin-1-yl)-4-oxoquinazolin-3(4H)-yl]benzamide (AZD6703), a clinical p38alpha MAP kinase inhibitor for the treatment of inflammatory diseases, *Bioorg. Med. Chem. Lett.* 22 (2012) 3879–3883.
- [29] N.P. McLaughlin, P. Evans, M. Pines, The chemistry and biology of febrifugine and halofuginone, *Bioorg. Med. Chem.* 22 (2014) 1993–2004.
- [30] A.M. Alafeefy, A.E. Ashour, O. Prasad, L. Sinha, S. Pathak, F.A. Alasmari, A.K. Rishi, H.A. Abdel-Aziz, Development of certain novel N-(2-(2-oxoindolin-3-ylidene)hydrazinocarbonyl)phenyl)-benzamides and 3-(2-oxoindolin-3-ylideneamino)-2-substituted quinazolin-4(3H)-ones as CFM-1 analogs: design, synthesis, QSAR analysis and anticancer activity, *Eur. J. Med. Chem.* 92 (2015) 191–201.
- [31] M. Mahdavi, K. Pedrood, M. Safavi, M. Saeedi, M. Pordeli, S.K. Ardestani, S. Emami, M. Adib, A. Foroumadi, A. Shafiee, Synthesis and anticancer activity of N-substituted 2-arylquinazolinones bearing trans-stilbene scaffold, *Eur. J. Med. Chem.* 95 (2015) 492–499.
- [32] S. Yin, L. Zhou, J. Lin, L. Xue, C. Zhang, Design, synthesis and biological activities of novel oxazol[4,5-g]quinazolin-2(1H)-one derivatives as EGFR inhibitors, *Eur. J. Med. Chem.* 101 (2015) 462–475.
- [33] J. Stamos, M.X. Sliwkowski, C. Eigenbrot, Structure of the epidermal growth factor receptor kinase domain alone and in complex with a 4-anilinoquinazoline inhibitor, *J. Biol. Chem.* 277 (2002) 46265–46272.
- [34] G. Marzaro, A. Guiotto, A. Chilin, Quinazoline derivatives as potential anti-cancer agents: a patent review (2007–2010), *Expert. Opin. Ther. Pat.* 22 (2012)

- 223–252.
- [35] S. Ravez, O. Castillo-Aguilera, P. Depreux, L. Goossens, Quinazoline derivatives as anticancer drugs: a patent review (2011–present), *Expert. Opin. Ther. Pat.* 25 (2015) 789–804.
- [36] A. Chilin, G. Marzaro, S. Zanatta, A. Guiotto, A microwave improvement in the synthesis of the quinazoline scaffold, *Tetrahedron Lett.* 48 (2007) 3229–3231.
- [37] X.M. Ou, W.C. Li, D.S. Liu, Y.P. Li, F.Q. Wen, Y.L. Feng, S.F. Zhang, X.Y. Huang, T. Wang, K. Wang, X. Wang, L. Chen, VEGFR-2 antagonist SU5416 attenuates bleomycin-induced pulmonary fibrosis in mice, *Int. Immunopharmacol.* 9 (2009) 70–79.
- [38] B.C. Fuchs, Y. Hoshida, T. Fujii, L. Wei, S. Yamada, G.Y. Lauwers, C.M. McGinn, D.K. DePeralta, X. Chen, T. Kuroda, M. Lanuti, A.D. Schmitt, S. Gupta, A. Crenshaw, R. Onofrio, B. Taylor, W. Winckler, N. Bardeesy, P. Caravan, T.R. Golub, K.K. Tanabe, Epidermal growth factor receptor inhibition attenuates liver fibrosis and development of hepatocellular carcinoma, *Hepatology* 59 (2014) 1577–1590.
- [39] N. Lin, S. Chen, W. Pan, L. Xu, K. Hu, R. Xu, NP603, a novel and potent inhibitor of FGFR1 tyrosine kinase, inhibits hepatic stellate cell proliferation and ameliorates hepatic fibrosis in rats, *Am. J. Physiol. Cell Physiol.* 301 (2011) C469–C477.
- [40] E. Karimizadeh, N. Motamed, M. Mahmoudi, S. Jafarinejad-Farsangi, A. Jamshidi, H. Faridani, F. Gharibdoost, Attenuation of fibrosis with selective inhibition of c-Abl by siRNA in systemic sclerosis dermal fibroblasts, *Arch. Dermatol. Res.* 307 (2014) 135–142.
- [41] J.H. Distler, O. Distler, Intracellular tyrosine kinases as novel targets for anti-fibrotic therapy in systemic sclerosis, *Rheumatol. Oxf.* 47 (Suppl. 5) (2008) v10–11.
- [42] G. Son, I.N. Hines, J. Lindquist, L.W. Schrum, R.A. Rippe, Inhibition of phosphatidylinositol 3-kinase signaling in hepatic stellate cells blocks the progression of hepatic fibrosis, *Hepatology* 50 (2009) 1512–1523.
- [43] D. Shegogue, M. Trojanowska, Mammalian target of rapamycin positively regulates collagen type I production via a phosphatidylinositol 3-kinase-independent pathway, *J. Biol. Chem.* 279 (2004) 23166–23175.
- [44] Y. Liu, X.M. Wen, E.L. Lui, S.L. Friedman, W. Cui, N.P. Ho, L. Li, T. Ye, S.T. Fan, H. Zhang, Therapeutic targeting of the PDGF and TGF-beta-signaling pathways in hepatic stellate cells by PTK787/ZK22258, *Lab. Invest.* 89 (2009) 1152–1160.
- [45] J.R. Hecht, T. Trarbach, J.D. Hainsworth, P. Major, E. Jager, R.A. Wolff, K. Lloyd-Salvant, G. Bodoky, K. Pendergrass, W. Berg, B.L. Chen, T. Jalava, G. Meinhardt, D. Laurent, D. Leibold, D. Kerr, Randomized, placebo-controlled, phase III study of first-line oxaliplatin-based chemotherapy plus PTK787/ZK 222584, an oral vascular endothelial growth factor receptor inhibitor, in patients with metastatic colorectal adenocarcinoma, *J. Clin. Oncol.* 29 (2011) 1997–2003.
- [46] V. Ankoma-Sey, M. Matli, K.B. Chang, A. Lalazar, D.B. Donner, L. Wong, R.S. Warren, S.L. Friedman, Coordinated induction of VEGF receptors in mesenchymal cell types during rat hepatic wound healing, *Oncogene* 17 (1998) 115–121.
- [47] Y. Liu, E.L. Lui, S.L. Friedman, L. Li, T. Ye, Y. Chen, R.T. Poon, J. Wo, T.W. Kok, S.T. Fan, PTK787/ZK22258 attenuates stellate cell activation and hepatic fibrosis in vivo by inhibiting VEGF signaling, *Lab. Invest.* 89 (2009) 209–221.
- [48] M. Varela-Rey, C. Montiel-Duarte, J.A. Osés-Prieto, M.J. Lopez-Zabalza, J.P. Jaffrezou, M. Rojkind, M.J. Iraburu, p38 MAPK mediates the regulation of alpha1(I) procollagen mRNA levels by TNF-alpha and TGF-beta in a cell line of rat hepatic stellate cells(1), *FEBS Lett.* 528 (2002) 133–138.
- [49] C. Yin, K.J. Evason, K. Asahina, D.Y. Stainier, Hepatic stellate cells in liver development, regeneration, and cancer, *J. Clin. Invest.* 123 (2013) 1902–1910.
- [50] S.P. Yun, S.J. Lee, Y.H. Jung, H.J. Han, Galectin-1 stimulates motility of human umbilical cord blood-derived mesenchymal stem cells by downregulation of smad2/3-dependent collagen 3/5 and upregulation of NF-kappa B-dependent fibronectin/laminin 5 expression, *Cell Death Dis.* 5 (2014).
- [51] S. Al Saleh, L.H. Sharaf, Y.A. Luqmani, Signalling pathways involved in endocrine resistance in breast cancer and associations with epithelial to mesenchymal transition (Review), *Int. J. Oncol.* 38 (2011) 1197–1217.
- [52] E.F. Pettersen, T.D. Goddard, C.C. Huang, G.S. Couch, D.M. Greenblatt, E.C. Meng, T.E. Ferrin, UCSF, Chimera—a visualization system for exploratory research and analysis, *J. Comput. Chem.* 25 (2004) 1605–1612.
- [53] Marvin, Version 5.5.0.1, Program B; ChemAxon: Budapest, Hungary; www.chemaxon.com/products (accessed 05/01/2015).
- [54] N.M. O'Boyle, M. Banck, C.A. James, C. Morley, T. Vandermeersch, G.R. Hutchison, Open Babel: an open chemical toolbox, *J. Cheminform* 3 (2011) 33.
- [55] G.M. Morris, R. Huey, W. Lindstrom, M.F. Sanner, R.K. Belew, D.S. Goodsell, A.J. Olson, AutoDock4 and AutoDockTools4: automated docking with selective receptor flexibility, *J. Comput. Chem.* 30 (2009) 2785–2791.
- [56] P. Brun, I. Castagliuolo, M. Pinzani, G. Palu, D. Martines, Exposure to bacterial cell wall products triggers an inflammatory phenotype in hepatic stellate cells, *Am. J. Physiol. Gastrointest. Liver Physiol.* 289 (2005) G571–G578.